



Article

Novel $\text{K}_2\text{Ti}_8\text{O}_{17}$ Anode via $\text{Na}^+/\text{Al}^{3+}$ Co-Intercalation Mechanism for Rechargeable Aqueous Al-Ion Battery with Superior Rate Capability

Qiangqiang Feng ^{1,†}, Yanyan Liu ^{1,*,†}, Jitong Yan ¹, Wei Feng ¹, Shaozheng Ji ^{2,3} and Yongfu Tang ^{1,*}

¹ Hebei Key Laboratory of Applied Chemistry, College of Environmental and Chemical Engineering, Yanshan University, Qinhuangdao 066004, China; f2394713046@163.com (Q.F.); yanjitong@outlook.com (J.Y.); fw980240907@163.com (W.F.)

² Materials and Nano Physics, School of Engineering Sciences, KTH Royal Institute of Technology, SE-100 44 Stockholm, Sweden; jshaoz@kth.se

³ School of Physics, Ultrafast Electron Microscopy Laboratory, Nankai University, Tianjin 300071, China

* Correspondence: liuyy@ysu.edu.cn (Y.L.); tangyongfu@ysu.edu.cn (Y.T.)

† These authors make equal contributions.

1. Supplementary Figures

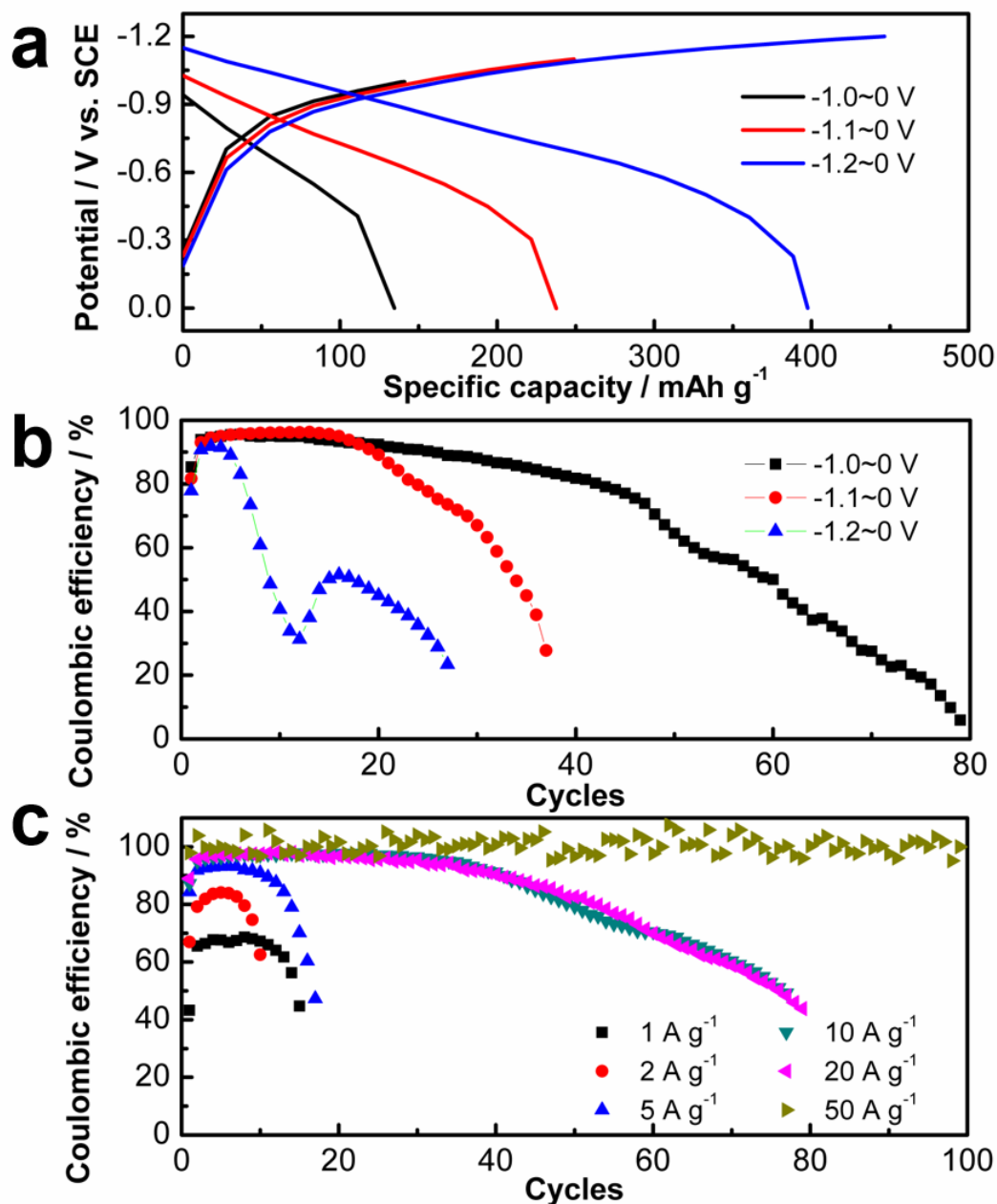


Figure S1. Electrochemical performance of $K_2Ti_8O_{17}$ electrode in the 1 M $AlCl_3$ aqueous solution. (a) GCD curves at different potential ranges with sweep rate of 10 mV s⁻¹. (b) Coulombic efficiencies based on the GCD curves with a current density of 10 A g⁻¹ at different potential ranges. (c) Discharge efficiencies based on the GCD curves at different current densities with a potential range of -1~0 V_{vs} SCE.

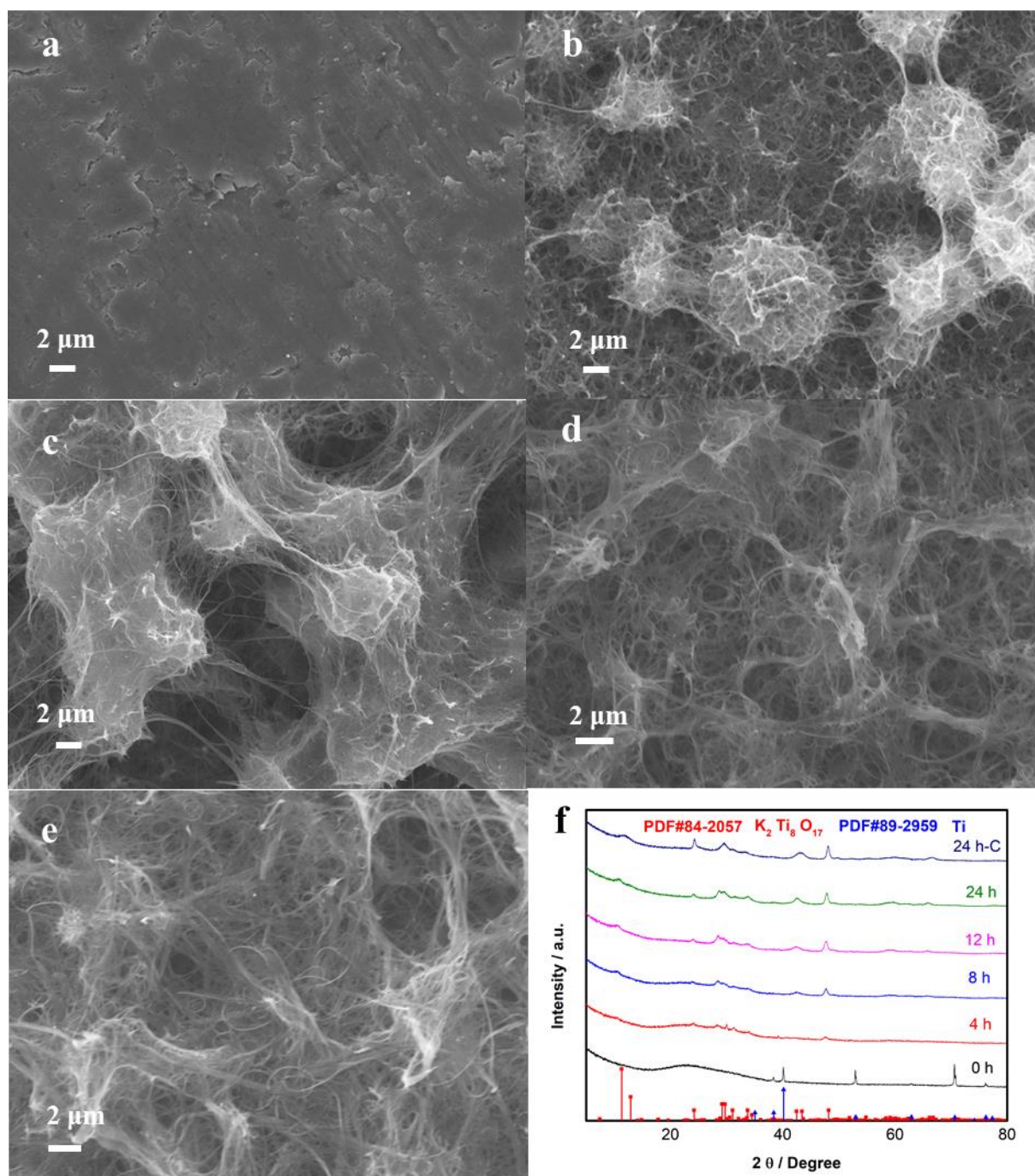


Figure S2. The morphology evolution process of $K_2Ti_8O_{17}$ electrode with the hydrothermal reaction times: (a) 0 h, (b) 4 h, (c) 8 h, (d) 12 h, (e) 24 h, and (f) the XRD patterns of the $K_2Ti_8O_{17}$ samples with different hydrothermal reaction times.

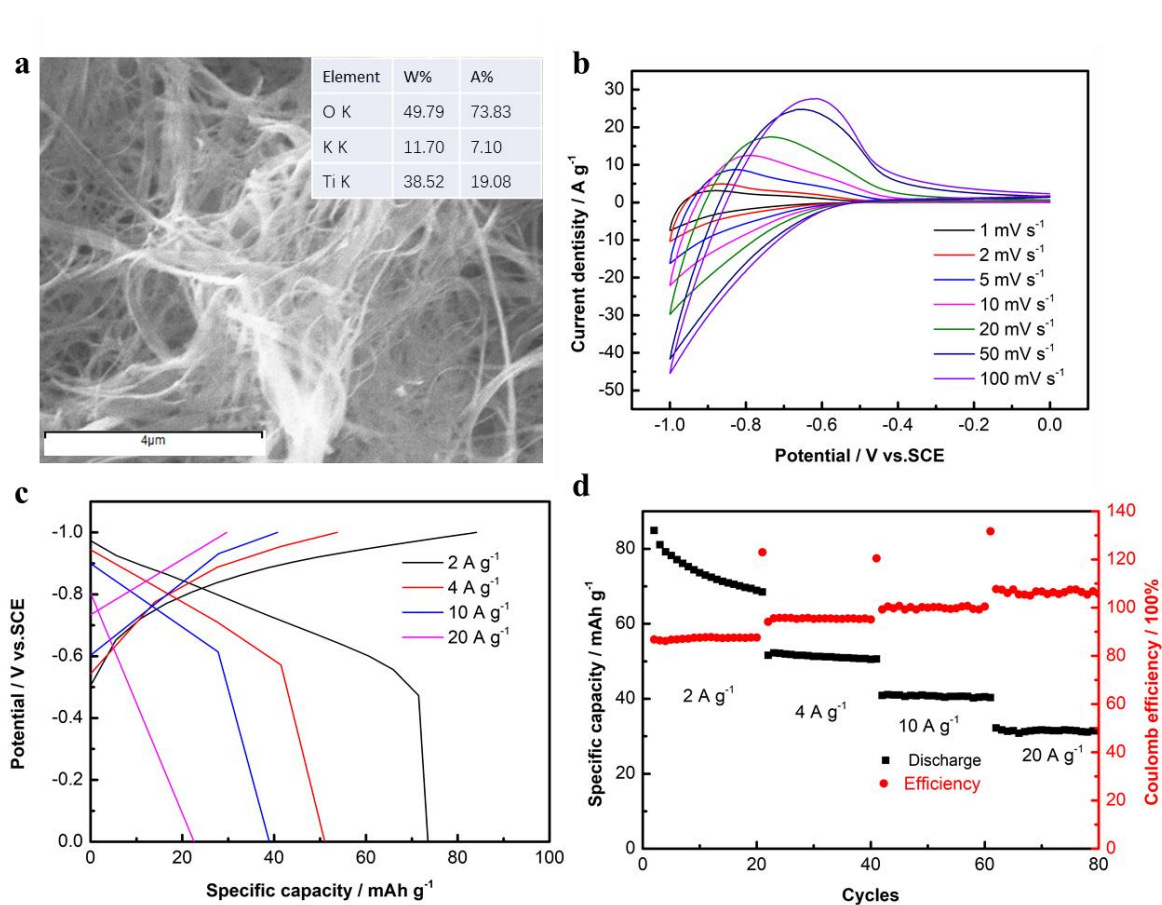


Figure S3. (a) The SEM and EDS results of the $\text{K}_2\text{Ti}_8\text{O}_{17}$ sample suffering a 24 h hydrothermal process before pyrolysis step. The electrochemical measurements of $\text{K}_2\text{Ti}_8\text{O}_{17}$ electrode in AlCl_3 electrolyte: (b) CV curves at different scan rates, (c) GCD curves at different current densities, (d) rate performance.

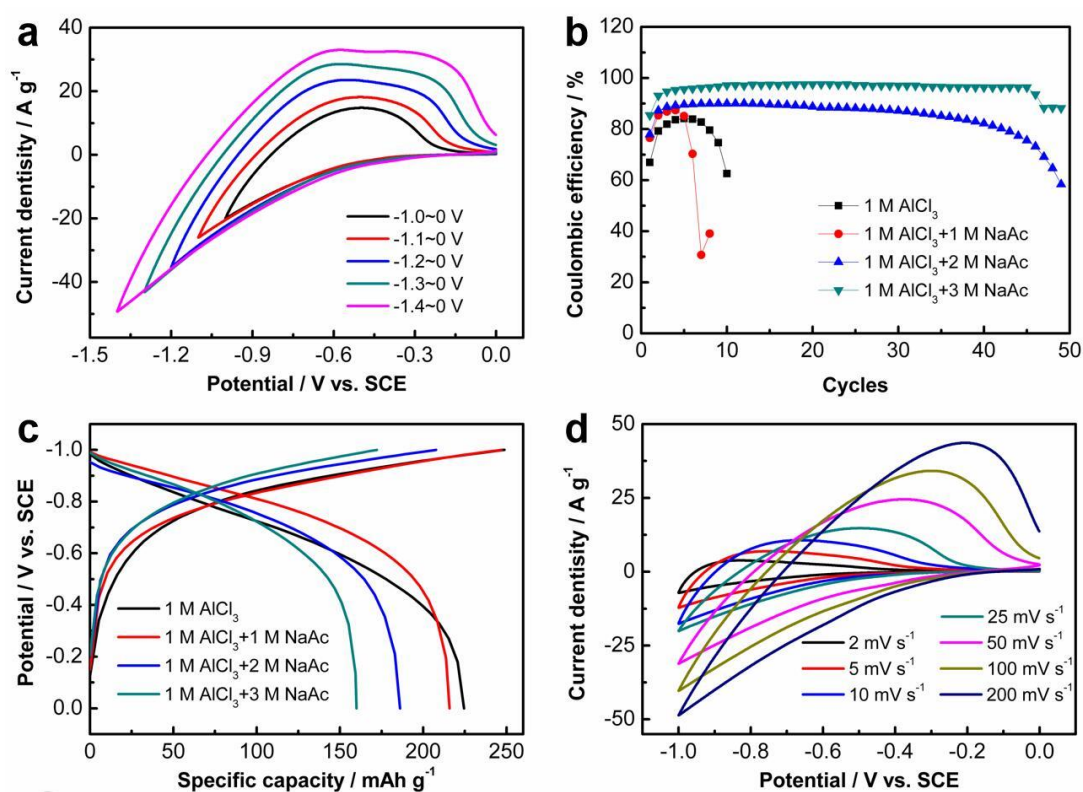


Figure S4. Electrochemical performance of $K_2Ti_8O_{17}$ electrode in the $AlCl_3/NaAc$ aqueous electrolyte. (a) CV curves at different potential ranges with scan rate of 10 mV s^{-1} . (b) CV curves with different scan rates at the potential range of -1 ~ 0 V vs SCE; Coulombic efficiencies based on the GCD curves with current density of 10 A g^{-1} at different potential ranges. (c) Coulombic efficiencies based on the GCD curves at different current densities with a potential range of -1~0 V vs SCE. (d) the CV curves at various scan rates.

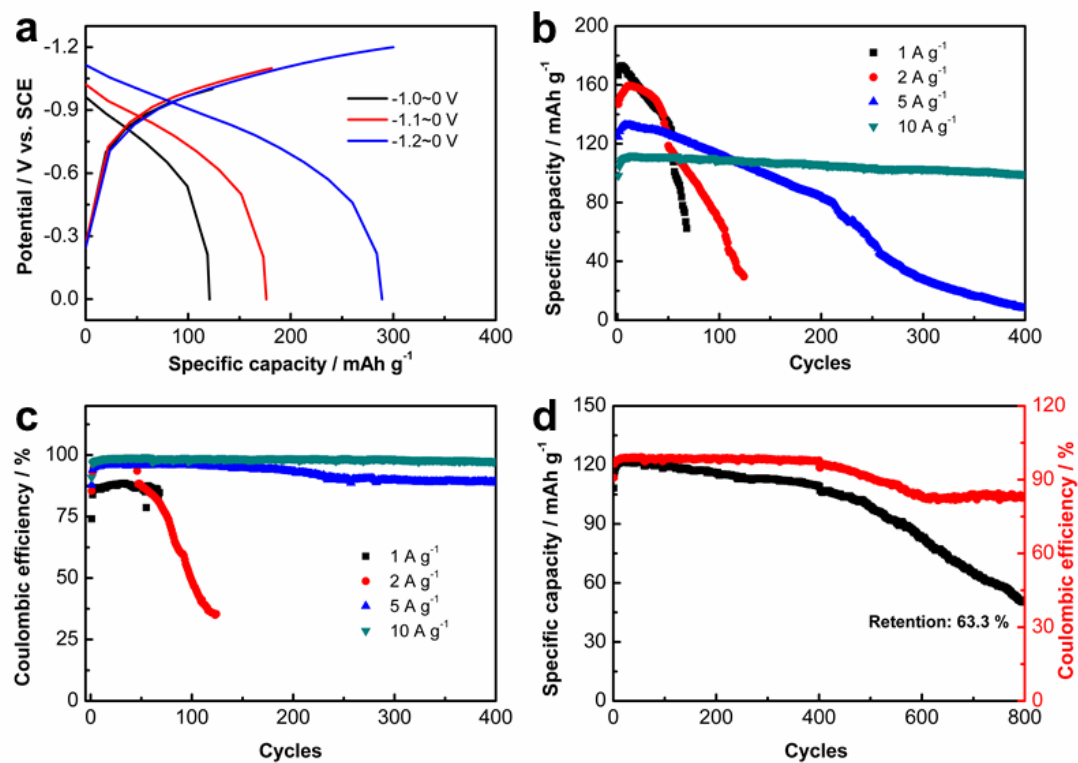


Figure S5. (a) Charge-discharge curves of $K_2Ti_8O_{17}$ electrode at different potential ranges at the current density of 10 A g^{-1} . (b) Cycling performances and (c) CEs of the $K_2Ti_8O_{17}$ electrode at different current densities. (d) Cycling performance of $K_2Ti_8O_{17}$ electrode at the current density of 10 A g^{-1} .

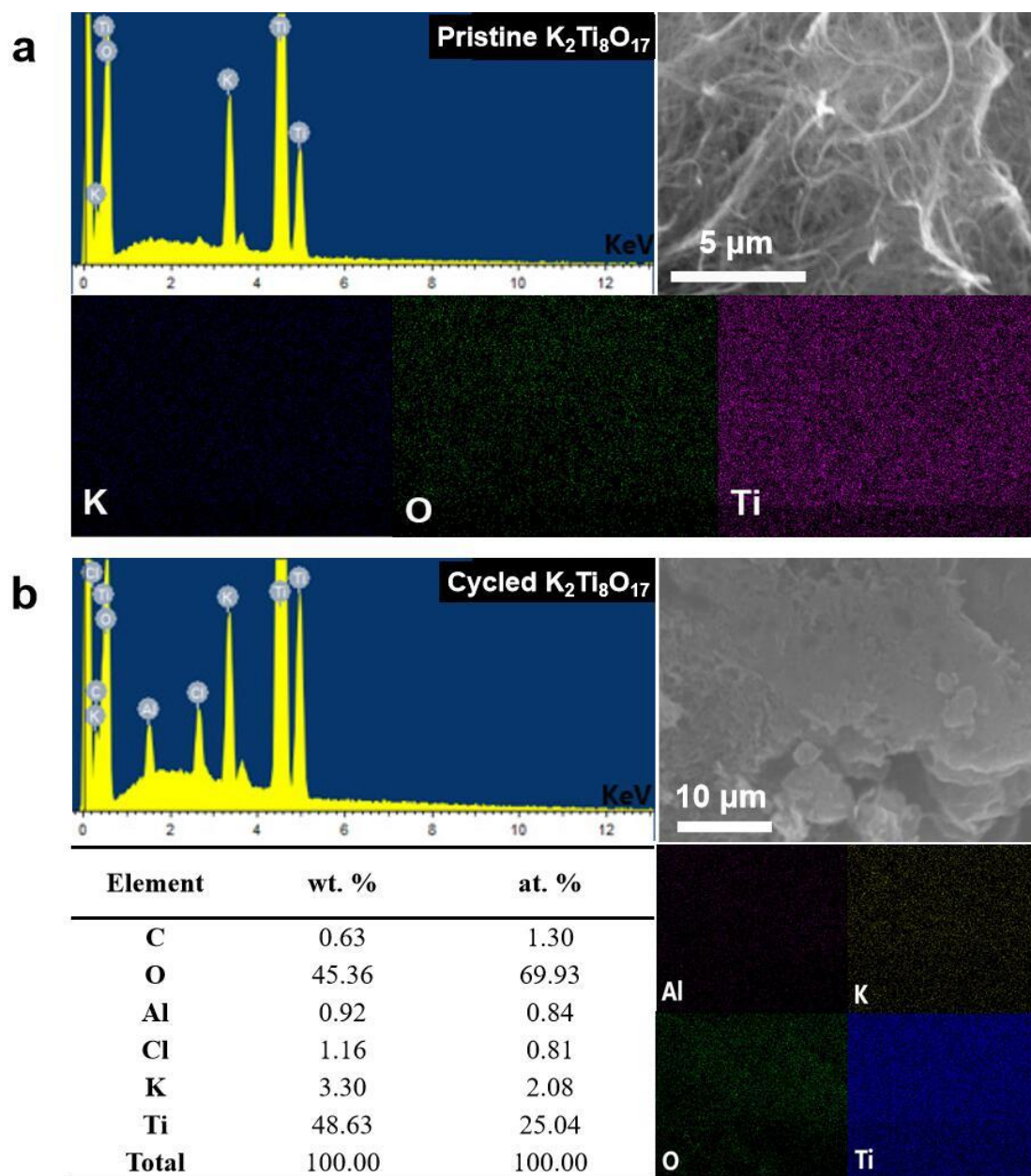


Figure S6. (a) EDX energy spectrum and element distribution of the pristine $K_2Ti_8O_{17}$. (b) EDX spectrum and element distribution diagram of electrode after 400 cycles of current density of $10 A g^{-1}$ in $AlCl_3/NaAc$ aqueous electrolyte.

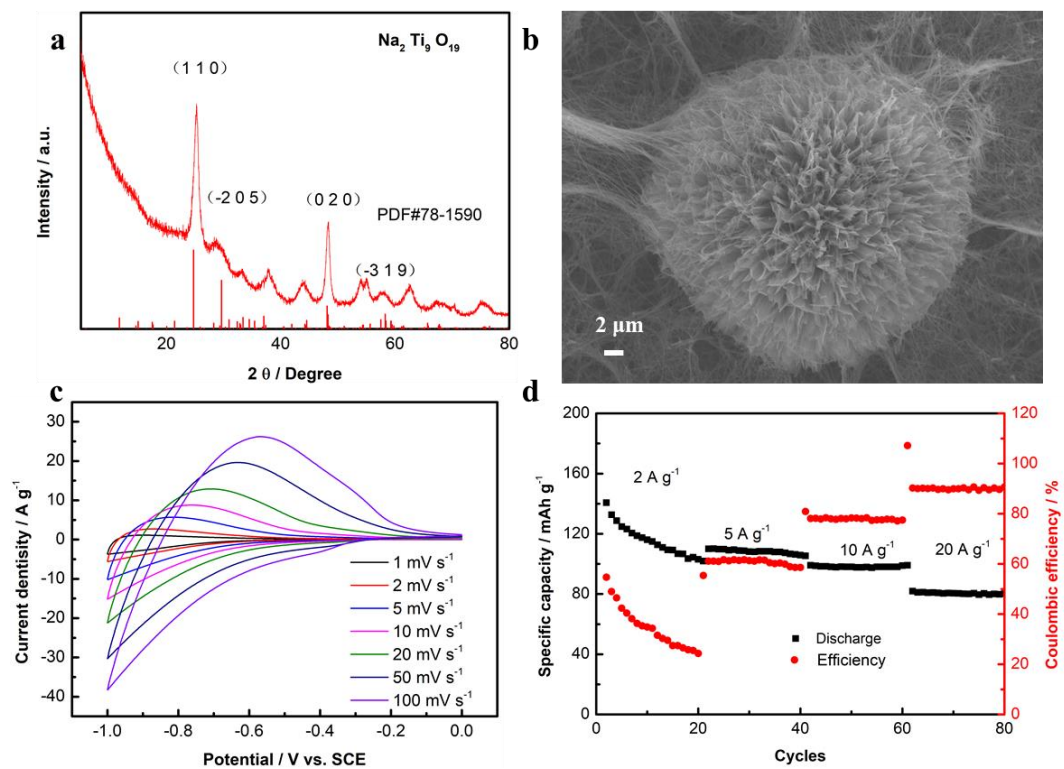


Figure S7. The physical characterizations and electrochemical performance of $\text{Na}_2\text{Ti}_9\text{O}_{19}$ sample: (a) XRD pattern, (b) SEM image, (c) CV curves at different scan rates, and (d) rate capacity and CEs.

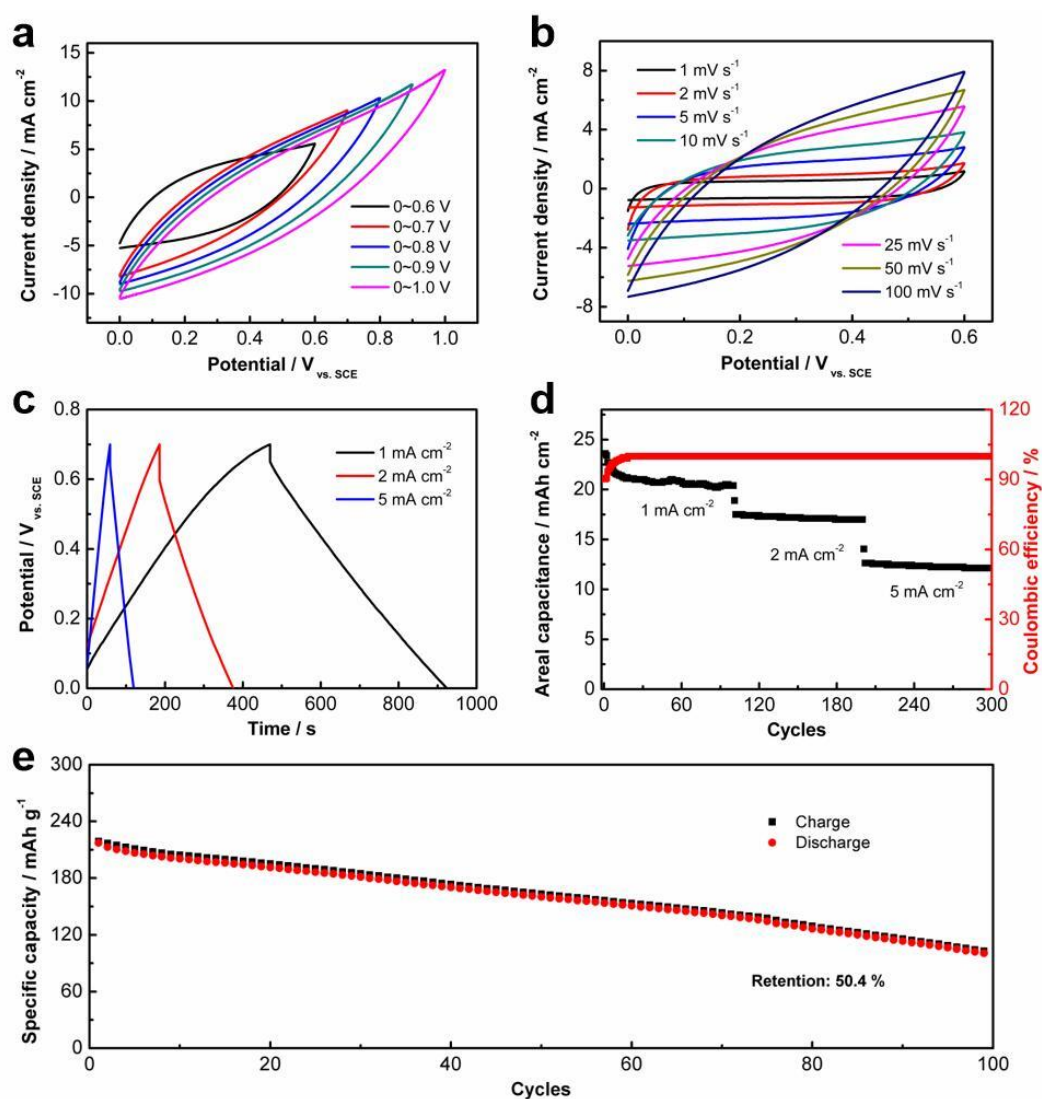


Figure S8. (a) CV curves of the AC coated on Ti mesh (AC-Ti) electrode at different potential ranges with Table 25. mV s⁻¹. (b) CV curves of AC-Ti electrode with different scan rates at the potential range of 0~0.6 V. (c) GCD curves of the AC-Ti electrode at different current densities. (d) Rate-performance and (e) cycling stability of the AC-Ti electrode at different current densities at the potential range of 0~0.7 V.

2. Supplementary Table

Table S1. The ratio of the peak intensities of the $e_g(L_3)/t_{2g}(L_3)$ in $K_2Ti_8O_{17}$ electrode.

Electrode	$K_2Ti_8O_{17}$	Discharge	Charge
$e_g(L_3)/t_{2g}(L_3)$	3.3590	3.3149	3.4906